Measurement of the annihilation decay rate of $2\,^3S_1$ positronium

R. E. Sheldon, T. J. Babij, B. A. Devlin-Hill, L. Gurung, D. B. Cassidy

Department of Physics and Astronomy, University College London, Gower Street, London, WC1E 6BT, UK

PACS 36.10.Dr – Positronium
PACS 31.50.Df – Excited states, atomic spectra
PACS 32.70.Cs – Lifetimes, atomic spectra

Abstract –We report a measurement of the annihilation decay rate of $2\,^3S_1$ positronium (Ps) atoms, $\Gamma_{exp}(2\,^3S_1)$. Ground state atoms optically excited to radiatively metastable $2\,^3S_1$ states were quenched via Stark mixing by the application of a time-delayed electric field. Rapid radiative decay of the Stark-mixed states to the ground state, followed by self-annihilation, was observed via the annihilation radiation time spectrum, and used to determine the number of excited state atoms remaining at different times, and hence the decay rate. We obtain $\Gamma_{exp}(2\,^3S_1) = 843 \pm 72$ kHz, in broad agreement with the Zeeman-shifted theoretical value of 890 kHz.

Introduction. – Immediately after Martin Deutsch first created Positronium (Ps) atoms in the laboratory in 1951 [1] he was able to measure the annihilation decay rate of the $1\,^3S_1$ triplet ground state [2]. At the time there were three extant calculations for this rate, suggesting values ranging from 1-7 MHz, and the measured value of 6.8±0.7 MHz was sufficient to demonstrate that the calculation of Ore and Powell [3] was correct. Since then several measurements of Ps annihilation decay rates for both singlet [4] and triplet [5] ground states have been performed [6]. A long-standing disagreement between theory and measurements for the triplet rate [7] has been resolved [8, 9], and the current experimental value for the triplet ground state decay rate is $\Gamma_{exp}(1\,^3S_1) = 7.0401 \pm 0.0007$ MHz [10].

Ps annihilation requires spatial overlap between the electron and positron wavefunctions, $\psi(r)$. Since these wavefunctions are hydrogenic, this overlap $|\psi(0)|^2$ is zero for states in which the orbital angular momentum quantum number $\ell \neq 0$ [11], and, for all practical purposes, one can assume that only $\ell = 0$ (S) states decay by annihilation [12]. Ps annihilation rates also depend on the spin configuration, because the number of gamma-ray photons (N) emitted in the process must satisfy charge conjugation invariance, which results in the selection rule [13] $(-1)^{\ell+S} = (-1)^N$, where S refers to the Ps spin quantum number. Accordingly, and taking into account energy and momentum conservation, two and three-photon emission are the dominant Ps annihilation decay modes for singlet and triplet states, respectively. The lowest order annihilation rates are

$$\Gamma_0(^1S_0) = \frac{\alpha^5 m_e c^2}{2\hbar n^3} = \frac{8.0325\ \text{GHz}}{n^3}, \tag{1}$$

and

$$\Gamma_0(^3S_1) = \frac{2}{9\pi}(\pi^2 - 9)\frac{\alpha^6 m_e c^2}{\hbar n^3} = \frac{7.2112\ \text{MHz}}{n^3}, \tag{2}$$

where $\Gamma_0(^1S_0)$ is the lowest order singlet decay rate [14] that can be obtained from the Dirac annihilation cross section [15], and $\Gamma_0(^3S_1)$ is the lowest order triplet decay rate first calculated by Ore and Powell [3]. Higher order QED corrections have been calculated [6] which, for the triplet case, yield a Ps decay rate of $\Gamma_{th}(1\,^3S_1) = 7.039971 \pm 0.000011$ MHz.

For pure S states, both radiative and annihilation decay rates scale with n^{-3}, and most excited Ps states will decay radiatively to lower lying states before annihilating. For example, $3\,^3S_1$ atoms will decay to $2\,^3P_J$ states with a mean radiative lifetime $\tau_{rad} \approx 300$ ns, whereas the mean $3\,^3S_1$ annihilation lifetime $\tau_{ann} \approx 4$ μs. The only excited states for which direct self-annihilation is a significant decay mechanism are the radiatively metastable $2\,^1S_0$ and $2\,^3S_1$ states [16], for which fluorescence decay is forbidden by electric dipole selection rules.

While the decay rates of the Ps ground states are well established experimentally [10], the excited state annihilation rates have not previously been measured. Here we report the first measurement of the annihilation rate of $2\,^3S_1$ atoms.

Experimental methods. – The positron beam, Ps production, laser excitation, and measurement methods used in this work are similar to those discussed elsewhere [17, 18]. A pulsed beam containing $\sim 10^6$ positrons/pulse with a Gaussian spatial (temporal) profile of approximately 2 mm (3 ns) (FWHM) was generated using a two-stage Surko-type buffer gas trap [19]. This beam was guided by an axial magnetic field ($B_z = 50$ G) and implanted into a mesoporous silica target [20] with an impact energy of 3.5 keV; Ps atoms created in the silica with energies of several eV were able to cool via collisions with internal surfaces and were emitted into vacuum with the zero-point energy of the confining voids, which, in the present case, is on the order of 50 meV [21].

Ps atoms were emitted from the silica target into vacuum within 5 ns of the positron implantation [22] and were subsequently irradiated with light from a pulsed ultraviolet (UV) dye laser, tuned to drive $1\,^3S_1 \rightarrow 2\,^3P_J$ transitions ($\lambda_{UV} = 243.02$ nm). For some measurements a second infrared (IR) dye laser ($\lambda_{IR} = 730 - 760$ nm) was also used to excite $n = 2$ atoms to Rydberg states, or to photoionize them [23]. The UV and IR laser beam widths were ≈ 3 and 6 mm, respectively so that all atoms excited by the UV laser were addressed by the IR laser.

The velocity distributions of Ps atoms emitted from silica targets are in general quite broad [21,24] which means that slower Ps profiles can be obtained by velocity selection techniques [25–27]. The most straightforward way to accomplish this is to delay the excitation laser pulse with respect to the incident positron pulse. Using a 20 ns delay with respect to the optimal excitation time we obtain excited Ps atoms with rms velocities in the x, y, and z directions of approximately 15, 50, and 85 km/s, respectively. This laser delay reduced the signal by approximately 40%. For excited state atoms v_x^{rms} was defined by the Doppler selection of the 100 GHz UV excitation laser [22], v_y^{rms}, was defined by collimation by the electrodes, and v_z^{rms} has been measured via Time of Flight (TOF) distributions in a Rydberg guiding experiment using the same silica film [28]. The velocity selection of excited atoms is dominated by the UV laser properties, and both Rydberg and metastable $2\,^3S_1$ atoms will have almost identical distributions [29].

Ps atoms in the $2\,^3S_1$ state were produced using a single-photon excitation technique [30] wherein ground state $1\,^3S_1$ atoms were optically excited to Stark mixed $2\,^3S'_1$ states in an electric field $F_{ex} = 2.7$ kV/cm, defined by the voltages applied to the target electrode V_T =-3.5kV and the grid electrode V_G =-400V, where the separation between these electrodes was 1.15 cm (see Fig. 1). NB: the -400V grid voltage was required to prevent backscattered positrons from interacting with the quenching electrodes and generating spurious timing signals. The target and grid voltages were turned off immediately after the UV laser pulse using a fast high voltage switch (90-10% turn off time = 60 ns), allowing some of the $2\,^3S'_1$ atoms to adiabatically evolve into pure $2\,^3S_1$ atoms, which were then

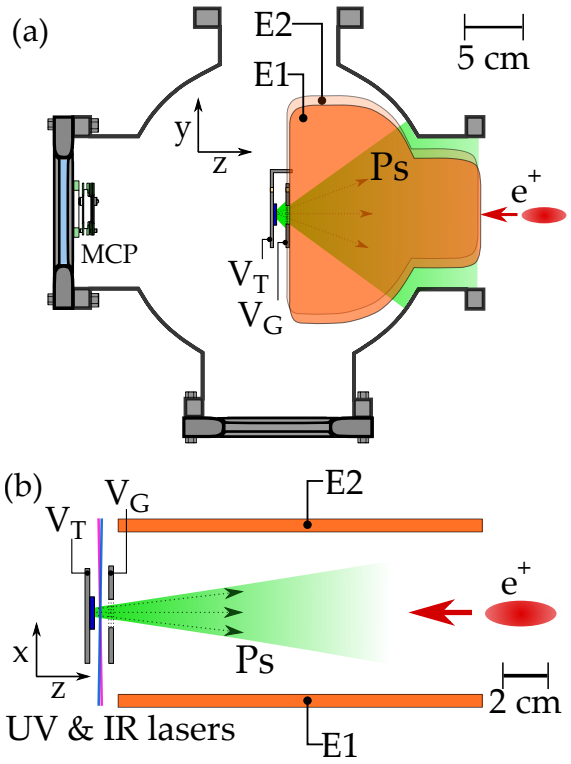

Fig. 1: (a) Schematic representation of the positronium production chamber, including the Ps excitation region (between the target electrode T and grid electrode G) and the quenching region (between electrodes E1 and E2), (b) top view of the quenching electrodes and laser-selected Ps trajectories. The target electrode bias V_T = -3.5 kV is switched off after Ps atoms have been excited by the laser pulse to $n = 2$ states. The grid electrode bias V_G, was -400V for $2\,^3S_1$ production, and is set to be the same as V_T for Rydberg production.

able to fly into the quenching region, between electrodes $E1$ and $E2$, as shown schematically in Fig. 1.

Ps annihilation radiation was observed using a single-shot technique [31] employing a γ-ray detector composed of a lutetium-yttrium oxyorthosilicate (LYSO) scintillator coupled to photomultiplier tube (PMT) [32]. This detector was connected to an oscilloscope used to record $V(t)$, the time-dependent detector anode voltage following a positron pulse, from which lifetime spectra were generated. The detector had an active area of 45 cm^2, and was placed approximately 35 cm from the Ps excitation region as indicated in Fig. 2. Examples of lifetime spectra obtained from this detector are shown in Fig. 3 (a).

The number of $2\,^3S_1$ atoms present as a function of time was determined by applying a time-delayed quenching electric field. This field resulted in $2\,^3S_1$ states becoming Stark mixed [12, 33, 34] and, just as the P character of these $2\,^3S'_1$ states allows then to be populated via direct single-photon excitation from the ground state [30], so too does it provide a radiative decay pathway to the ground state. The $1\,^3S_1$ ground state atoms will decay via three-photon self-annihilation at ≈ 7 MHz.

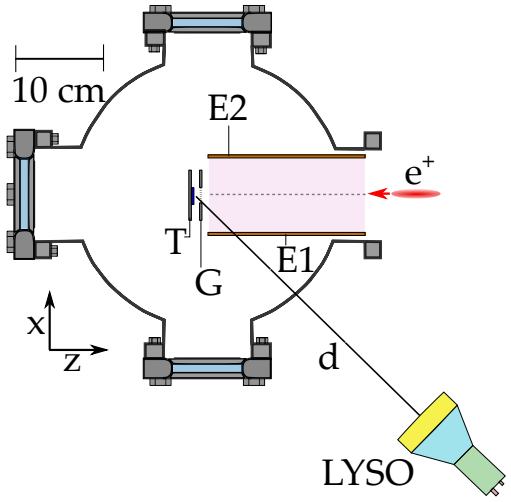

Fig. 2: Schematic representation of the Ps production chamber and the LYSO detector position, where d ≈35 cm.

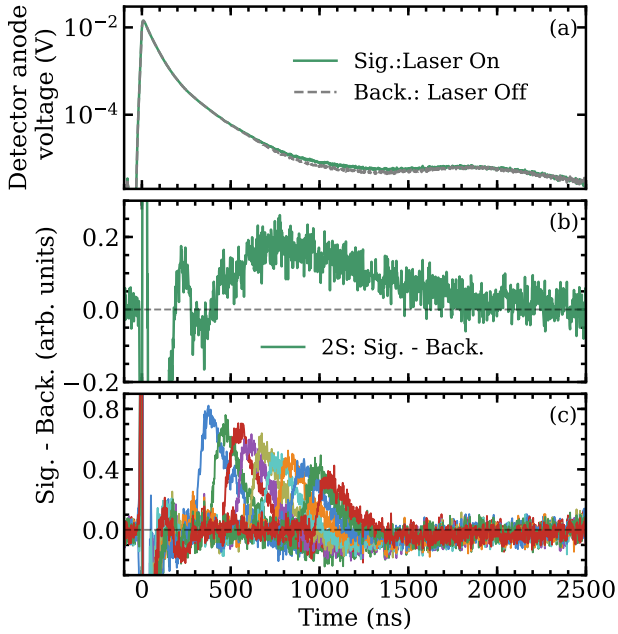

Fig. 3: (a) Example of single shot lifetime spectra recorded with and without Ps laser excitation, (b) difference spectra (laser on - laser off), showing a $2\,^3S_1$ signal, and (c) difference spectra showing a series of quenching peaks induced by turning on the quenching field at different times. The background signal in (b) is the case with no laser light present. The background signal in (c) is the $2\,^3S_1$ signal shown in (b). The data in (c) are the average of all lifetime measurements.

The slower, laser-selected, Ps speeds in the x direction made it possible to use quenching electrodes with a separation of 8.5 cm. This is an essential element of the experiment as it is currently configured because it simultaneously allows for long flight paths within a structure that can generate electric fields sufficient to quench $2\,^3S_1$ atoms, or to field ionize Rydberg atoms, without using excessively high voltages. The electric field was generated by applying -4kV to electrode $E1$ and +4kV to electrode $E2$ (see Fig. 1), generating a central field of ≈ 0.94 kV/cm. The electric field strength was not perfectly uniform across the entire volume in which $2\,^3S_1$ quenching is performed, but was sufficient to reduce the $2\,^3S'_1$ lifetime to less than 20 ns [30].

Additional measurements were performed using long-lived Rydberg atoms [35] as a control for variations in the detection efficiency and loss mechanisms other than spontaneous radiative decay. In order to maintain the positron beam impact energy, but also to produce Rydberg atoms in zero electric field, the target and grid biases V_T and V_G (see Fig. 1) were switched off after the positron implantation. Rydberg atoms with principal quantum number $n = 23$ were produced in a two-step excitation process [23]. The limited spectral resolution of this process did not allow precise selection of individual Stark states [29], but the laser width was such that the excitation was centered around states with relatively low Stark shifts (i.e., $k = 0$ states [36]). These states are expected to ionize at experimentally relevant rates in electric fields of ≈ 0.6 kV/cm [37]. Thus, the Rydberg atoms were fully ionized in the same electric fields used to quench $2\,^3S_1$ atoms. In the ionization process, liberated positrons were accelerated into the negatively charged electrode $E1$, leading mostly to annihilation [38], and generating a γ-ray pulse with an amplitude proportional to the number of ionized atoms. In both the quenching and ionization processes, the application of an electric field causes annihilation of long-lived atoms, and changes the time profile of the resulting annihilation radiation.

Single shot lifetime data are typically represented as the difference between "signal" and "background" spectra, where the background condition depends on what is being measured [17]. For example, Fig. 3 (b) shows difference spectra representing the production of $2\,^3S_1$ atoms, where the background spectra were recorded with no laser light present. In this case the long lifetime of $2\,^3S_1$ atoms compared to the $1\,^3S_1$ states results in an increased annihilation signal at later times. When the quenching field is applied the annihilation signal exhibits a corresponding peak caused by the field-induced increase in the population of shorter-lived ground state atoms, as shown in Fig. 3 (c).

The present measurement is based on periodically sampling the remaining population of $2\,^3S_1$ atoms via quenching. However, in addition to spontaneous decay events, the observed number of remaining atoms could be modified by two other processes, namely (1) atom collisions with the vacuum chamber walls or electrodes, and (2) variations in the γ-ray detection efficiency that depend on where the annihilation event takes place. The former arise because the atoms have a broad distribution of velocities, and some are able to collide with material objects before spontaneous emission can take place.

The second loss mechanism occurs because annihilation events take place in different locations, spread out over a relatively large area, owing to the long lifetimes and high speeds of the atoms, and the solid angle subtended by the detector relative to these positions is not constant. The relevant annihilation region has an area on the order of 100 cm^2 in the $y-z$ plane, (with a less significant displacement in the x direction). To achieve complete coverage of the long-lived Ps atoms would require a detector, with a solid angle subtending an area as large as the annihilation region. This could not be achieved using our standard scintillator-PMT based systems [32]. Smaller detectors will exhibit a detection efficiency that depends on where the annihilation events occur. This effect can be reduced if the detector is located far away, which is why the LYSO detector used in this work was placed ≈ 35 cm from the Ps formation region (see Fig. 2). Although this mitigates the position dependent detection efficiency, there is no detector position that can fully eliminate this problem without an unacceptable reduction in the count rate. The position of the LYSO detector was such that the average (geometric) detection efficiency was $\approx 1\%$, which nevertheless still leads to variations in the effective solid angle of more than 10% over the entire annihilation region.

Both collisional losses and variations in the detection efficiency were directly measured using highly-excited Rydberg atoms, for which the annihilation process can essentially be switched off. Ps atoms excited to states with principal quantum number $n = 23$ exhibit negligible self-annihilation, and with a fluorescence lifetime of more than 50 μs [35] also experience negligible radiative decay on the μs time scale of the measurements. Thus, these atoms can be used to isolate non-radiative loss mechanisms, either real (via collisions), or apparent (via variations in the detection efficiency).

Measurements of time-dependent electric field ionization of Rydberg atoms are shown in Fig. 4. These data were smoothed, using the Hamming method [39], with a 60 ns wide window, and then used to determine $A_{\mathrm{Ryd}}(t)$, the (normalized) Rydberg peak amplitudes obtained at different quenching times. It is evident that the first two peaks are lower in amplitude, and have longer tails, than the later peaks. The reason for this is that some of the slower atoms take longer than 300 ns to pass through the grid electrode and therefore are not quenched when the field is applied. This effect is exacerbated by the fact that there is a region of lower electric field strength just after the grid electrode. This means that at early times the ionization of some atoms will be delayed relative to the time at which the fields are switched on, giving rise to a peak with a lower amplitude, but a longer tail. These data indicate that ionization peaks measured at times before ≈ 486 ns will be missing some (unknown) fraction of atoms that are either not ionized, or are ionized at later times. Similarly, some $2\,^3\mathrm{S}_1$ atoms will also not be fully quenched at these times, and are therefore not included in fits to lifetime spectra (this constitutes the first two measured points).

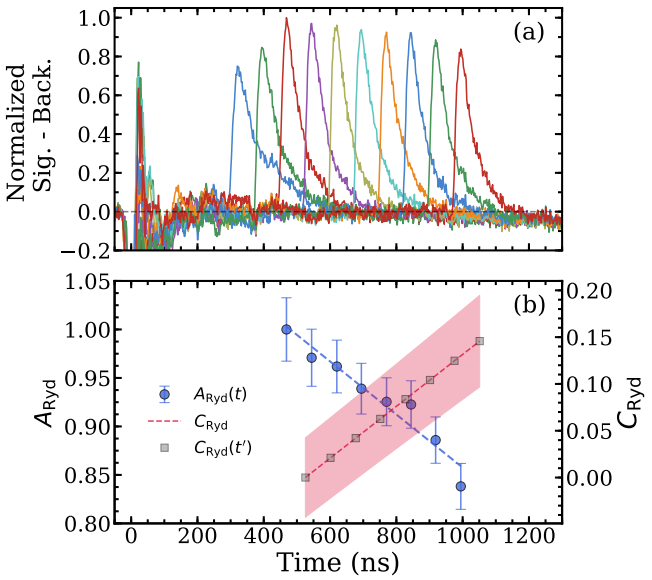

Fig. 4: (a) Rydberg electric field ionization data, normalized to the amplitude maximum of the third peak (at 486 ns), and (b) the normalized Rydberg peak amplitudes $A_{\mathrm{Ryd}}(t)$ and corresponding time-shifted correction factors, $C_{\mathrm{Ryd}}(t')$, derived from a linear fit (dashed line) to the data, as described in the text. The shaded bar represents the C_{Ryd} error obtained from the fit.

The $2\,^3\mathrm{S}_1$ quenching data were adjusted using the measured Rydberg data. In order to do this the different time scales of the ionization and quenching processes had to be taken into account. Rydberg atoms in the appropriate electric fields were ionized essentially instantaneously [37], whereas $2\,^3\mathrm{S}_1$ atoms first decay to the ground state, and then annihilate (at a rate of 7 MHz). This means that, before they finally annihilate, $2\,^3\mathrm{S}_1$ atoms will have moved relative to the corresponding ionized Rydberg atoms, and hence the solid angle and collision correction needed for these decay events will be slightly different. The quenching peak amplitudes $A_{\mathrm{meas}}(t')$ [see Fig. 3 (c)] were evaluated at time t', and the offset time $T = t' - t$ was determined by finding the time of each quenching peak maximum t^{max} relative to the corresponding Rydberg peak t^{Ryd}, and taking the average for all $(N-2)$ peaks used. That is,

$$T = \frac{1}{(N-2)} \sum_{i=3}^{N} (t_i^{\mathrm{max}} - t_i^{\mathrm{Ryd}}). \tag{3}$$

This time difference was accounted for by performing a linear fit to the Rydberg amplitude data to obtain the corresponding normalized Rydberg amplitude values $A_{\mathrm{Ryd}}(t')$ at the appropriate times (i.e., at t'). The time-shifted Rydberg correction factors $C_{\mathrm{Ryd}}(t') = 1 - A_{\mathrm{Ryd}}(t')$ obtained in this way are shown in Fig. 4 (b), where the error band comes from the fit error.

Results and Discussion. – The goal of the experiments described here was to measure the annihilation decay rate of radiatively metastable $2\,^3S_1$ Ps. This was achieved by optically exciting atoms to this level, and then periodically probing the population using a time-delayed quenching electric field. Lifetime spectra were generated by measuring the amplitudes of the field-induced annihilation peaks as indicated in Fig. 5 (a). This figure shows quenching data similar to those shown in Fig. 3 (c), with a Hamming smoothing procedure [39] (using a 60 ns wide window) applied to the difference spectra used to obtain the peak amplitudes $A_{\rm meas}(t')$. These amplitudes were used to generate uncorrected lifetime spectra, as shown in Fig. 5 (b). The quenching data were adjusted using the Rydberg data to obtain corrected amplitudes $A_{\rm corr}(t')$, such that

$$A_{\rm corr}(t') = A_{\rm meas}(t') + A^{\rm max}_{\rm meas} \times C_{\rm Ryd}(t'), \qquad (4)$$

where $A^{\rm max}_{\rm meas}$ is the amplitude of the first peak used in the fitting (i.e., at $t = 526$ ns in Fig. 5 (b)). This procedure gives the correction for the solid angle and collision variations, but does not account for the self-annihilation component of the correction fraction. However, trajectory simulations similar to those used previously [28] that include self-annihilation indicate that fewer than 5% of atoms are lost in this way, and that this introduces errors that are much smaller than the statistical errors already present in the correction factor. The corrected amplitude values were also used to generate lifetime spectra, as shown in Fig. 5 (b). For this particular run (number 6), an exponential fit to the uncorrected spectrum yields a lifetime of 712 ± 87 ns, which becomes 1107 ± 204 ns after the correction is applied.

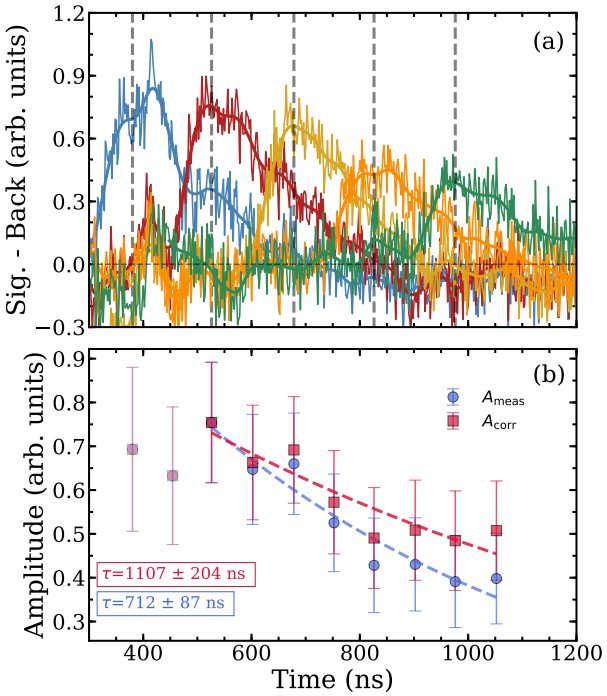

Fig. 5: (a) Quenching peaks with smoothing and (b) corresponding lifetime spectrum with and without the Rydberg correction for run number 6. The vertical dashed lines in (a) represent the times at which the peak amplitudes are evaluated, and the dashed lines in (b) are exponential fits to the data from which the lifetime is obtained. For clarity only alternate quenching peaks are shown in (a). The first two (gray) points in (b) were not included in the exponential fit, as discussed in the text.

A total of six separate measurements, similar to that shown in Fig. 5, were performed, with a total data acquisition time of 166 hours. The individual decay rates (where the decay rate is simply the inverse of the lifetime) obtained are shown in Fig. 6, as well as their weighted average. Each run has also been corrected according to the Rydberg data; the final average decay rate obtained from the entire corrected data set is $\Gamma_{\rm exp}(2\,^3S_1) = 843 \pm 72$ kHz.

This experiment by its nature suffers from low atom numbers and low detection efficiency, and hence the uncertainty is dominated by statistics, and systematic effects are negligible. The main systematic is Zeeman mixing between the $2\,^3S_1$ and $2\,^1S_0$ levels with $M_J = 0$. This increases the mean $2\,^3S_1$ decay rate from 880 to 890 kHz [12], which remains well within the statistical uncertainty of the measurement. Atoms that are not traveling perpendicular to the magnetic field will experience motional electric fields that lead to quenching of the $2\,^3S_1$ states [40, 41]. However, this effect is weak, and simulations taking into account the Ps velocity distributions [28] indicate a reduction in the lifetime on the order of 0.1%.

Our measurement of the $2\,^3S_1$ Ps decay rate is consistent with the expected 890 kHz from theory, but the ≈ 9 % precision is insufficient to test QED corrections to the lowest order decay rate calculation of Ore and Powell [3]. Nevertheless, it is the first time that the annihilation decay rate of an excited state of Ps has been measured, and we expect to be able to reduce the experimental uncertainties in future work.

The present measurement can be improved in several ways, most of which would be facilitated by using a source of colder Ps. Slower atoms would be beneficial because they can be excited more efficiently (using the single photon method), and allow for longer flight times without affecting detection efficiency. This would improve the statistics, and remove or reduce the need to correct for non-radiative losses. Unfortunately, no viable alternative options currently exist [18]. Thermal desorption sources can be employed (e.g., [42]), but, with the laser delayed Ps profiles, these are essentially equivalent to the Ps source used in this work. Colder Ps can be obtained from oxygen treated surfaces [43], but the stability of these surfaces in the presence of UV laser radiation makes this approach undesirable [44]. In the absence of colder atoms, more extreme velocity selection may improve the experiment, but would require more efficient γ-ray detection. This would be possible if a large detector array were employed; for a modular system with many small detector segments that

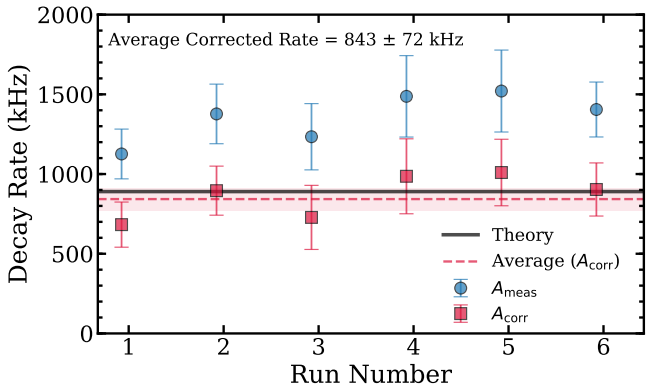

Fig. 6: Decay rates measured in all six runs, with and without the Rydberg correction. The solid horizontal line at 890 kHz is the Zeeman shifted theoretical $2\,^3S_1$ decay rate. The dashed horizontal line is the weighted average of all corrected data, and the shaded band around the average is the error.

record individual decay events [45], which would remove the need to correct for solid angle variations, and improve the overall detection efficiency.

Alternative $2\,^3S_1$ production methods may be considered; a two-photon Doppler-free excitation scheme [46] could be used, which would be up to five times more efficient [47], but this would not be compatible with an electrode structure designed for a narrow transverse velocity component. Single photon production via the $3\,^3P$ level is also possible [48], and may be ≈30% more efficient than the present method if stimulated emission is employed [49], although this would require more complex laser systems.

Conclusions. – We have performed the first measurement of the annihilation decay rate of $2\,^3S_1$ positronium. We obtain $\Gamma_{exp}(2\,^3S_1) = 843 \pm 72$ kHz, which is consistent with the (Zeeman shifted) theoretical value of 890 kHz [6]. The corresponding (Zeeman shifted) decay rate obtained from the lowest order calculation (see Eq 2) is ≈ 913 kHz [3], and the present measurement is therefore unable to test any QED corrections; a factor of 5 improvement in the precision would make it possible to test the first order QED corrections. By employing colder Ps atoms and more efficient detection, we estimate that a measurement using a similar methodology to that described here could reach the 1% level. By using a different detection scheme, with better time resolution than is possible with LYSO scintillators, this may become comparable to the precision achieved in ground state decay rate measurements, namely 100 ppm [10]. In that case a revised evaluation of the theoretical excited state decay rate may be needed, as some of the higher order corrections do not scale with n^3, meaning that $\Gamma_{th}(1\,^3S_1)$ cannot be directly scaled to find $\Gamma_{th}(2\,^3S_1)$ with high precision.

* * *

We gratefully acknowledge L. Liszkay for providing silica samples and G. S. Adkins for helpful discussions. This work was supported by the EPSRC under Grant No. EP/R006474/1).

REFERENCES

[1] Deutsch M 1951 *Phys. Rev.* **82**(3) 455–456 URL http://link.aps.org/doi/10.1103/PhysRev.82.455
[2] Deutsch M 1951 *Phys. Rev.* **83**(4) 866–867 URL http://link.aps.org/doi/10.1103/PhysRev.83.866
[3] Ore A and Powell J L 1949 *Phys. Rev.* **75**(11) 1696–1699 URL http://link.aps.org/doi/10.1103/PhysRev.75.1696
[4] Al-Ramadhan A H and Gidley D W 1994 *Phys. Rev. Lett.* **72**(11) 1632–1635 URL http://link.aps.org/doi/10.1103/PhysRevLett.72.1632
[5] Nico J S, Gidley D W, Rich A and Zitzewitz P W 1990 *Phys. Rev. Lett.* **65**(11) 1344–1347 URL https://link.aps.org/doi/10.1103/PhysRevLett.65.1344
[6] Adkins G S, Fell R N and Sapirstein J 2002 *Annals of Physics* **295** 136 – 193 ISSN 0003-4916 URL http://www.sciencedirect.com/science/article/pii/S0003491601962190
[7] Westbrook C I, Gidley D W, Conti R S and Rich A 1987 *Phys. Rev. Lett.* **58**(13) 1328–1331 URL https://link.aps.org/doi/10.1103/PhysRevLett.58.1328
[8] Vallery R S, Zitzewitz P W and Gidley D W 2003 *Phys. Rev. Lett.* **90**(20) 203402 URL http://link.aps.org/doi/10.1103/PhysRevLett.90.203402
[9] Jinnouchi O, Asai S and Kobayashi T 2003 *Physics Letters B* **572** 117 – 126 ISSN 0370-2693 URL http://www.sciencedirect.com/science/article/pii/S0370269303012607
[10] Kataoka Y, Asai S and Kobayashi T 2009 *Physics Letters B* **671** 219 – 223 ISSN 0370-2693 URL http://www.sciencedirect.com/science/article/pii/S0370269308014688
[11] Bethe H A and Salpeter E E 1957 *Quantum Mechanics of One- and Two-Electron Atoms* (Springer, Berlin)
[12] Alonso A M, Cooper B S, Deller A, Hogan S D and Cassidy D B 2016 *Phys. Rev. A* **93**(1) 012506 URL http://link.aps.org/doi/10.1103/PhysRevA.93.012506
[13] Wolfenstein L and Ravenhall D G 1952 *Phys. Rev.* **88**(2) 279–282 URL http://link.aps.org/doi/10.1103/PhysRev.88.279
[14] Wheeler J A 1946 *Annals of the New York Academy of Sciences* **48** 219–238 ISSN 1749-6632 URL http://dx.doi.org/10.1111/j.1749-6632.1946.tb31764.x
[15] Dirac P A M 1930 *Mathematical Proceedings of the Cambridge Philosophical Society* **26**(03) 361–375 ISSN 1469-8064 URL http://journals.cambridge.org/article_S0305004100016091
[16] Cooke D A, Crivelli P, Alnis J, Antognini A, Brown B, Friedreich S, Gabard A, Haensch T, Kirch K, Rubbia A and Vrankovic V 2015 *Hyperfine Interactions* 1–7 ISSN 0304-3843 URL http://dx.doi.org/10.1007/s10751-015-1158-4

[17] Cooper B S, Alonso A M, Deller A, Wall T E and Cassidy D B 2015 *Review of Scientific Instruments* **86** 103101 URL http://scitation.aip.org/content/aip/journal/rsi/86/10/10.1063/1.4931690

[18] Cassidy D B 2018 *The European Physical Journal D* **72** 53 ISSN 1434-6079 URL https://doi.org/10.1140/epjd/e2018-80721-y

[19] Danielson J R, Dubin D H E, Greaves R G and Surko C M 2015 *Rev. Mod. Phys.* **87**(1) 247–306 URL http://link.aps.org/doi/10.1103/RevModPhys.87.247

[20] Liszkay L, Corbel C, Perez P, Desgardin P, Barthe M F, Ohdaira T, Suzuki R, Crivelli P, Gendotti U, Rubbia A, Etienne M and Walcarius A 2008 *Appl. Phys. Lett.* **92** 063114 (pages 3)

[21] Cassidy D B, Crivelli P, Hisakado T H, Liszkay L, Meligne V E, Perez P, Tom H W K and Mills Jr A P 2010 *Phys. Rev. A* **81**(1) 012715

[22] Deller A, Cooper B S, Wall T E and Cassidy D B 2015 *New Journal of Physics* **17** 043059 URL http://stacks.iop.org/1367-2630/17/i=4/a=043059

[23] Cassidy D B, Hisakado T H, Tom H W K and Mills Jr A P 2012 *Phys. Rev. Lett.* **108**(4) 043401 URL http://link.aps.org/doi/10.1103/PhysRevLett.108.043401

[24] Crivelli P, Gendotti U, Rubbia A, Liszkay L, Perez P and Corbel C 2010 *Phys. Rev. A* **81**(5) 052703

[25] Cassidy D B, Hisakado T H, Meligne V E, Tom H W K and Mills Jr A P 2010 *Physical Review A* **82**(5) 052511

[26] Alonso A M, Cooper B S, Deller A, Gurung L, Hogan S D and Cassidy D B 2017 *Phys. Rev. A* **95**(5) 053409 URL https://link.aps.org/doi/10.1103/PhysRevA.95.053409

[27] Amsler C *et al* (The AEgIS Collaboration) 2019 *Phys. Rev. A* **99**(3) 033405 URL https://link.aps.org/doi/10.1103/PhysRevA.99.033405

[28] Rayment M H, Gurung L, Sheldon R E, Hogan S D and Cassidy D B 2019 *Phys. Rev. A* **100**(1) 013410 URL https://link.aps.org/doi/10.1103/PhysRevA.100.013410

[29] Wall T E, Alonso A M, Cooper B S, Deller A, Hogan S D and Cassidy D B 2015 *Phys. Rev. Lett.* **114**(17) 173001 URL http://link.aps.org/doi/10.1103/PhysRevLett.114.173001

[30] Alonso A M, Hogan S D and Cassidy D B 2017 *Phys. Rev. A* **95**(3) 033408 URL https://link.aps.org/doi/10.1103/PhysRevA.95.033408

[31] Cassidy D B, Deng S H M, Tanaka H K M and Mills Jr A P 2006 *Appl. Phys. Lett.* **88** 194105 (pages 3)

[32] Alonso A, Cooper B, Deller A and Cassidy D 2016 *Nuclear Instruments and Methods in Physics Research Section A: Accelerators, Spectrometers, Detectors and Associated Equipment* **828** 163 – 169 ISSN 0168-9002

[33] Alonso A M, Cooper B S, Deller A, Hogan S D and Cassidy D B 2015 *Phys. Rev. Lett.* **115**(18) 183401 URL http://link.aps.org/doi/10.1103/PhysRevLett.115.183401

[34] Aghion S *et al* (AEgIS Collaboration) 2018 *Phys. Rev. A* **98**(1) 013402 URL https://link.aps.org/doi/10.1103/PhysRevA.98.013402

[35] Deller A, Alonso A M, Cooper B S, Hogan S D and Cassidy D B 2016 *Phys. Rev. A* **93**(6) 062513 URL https://link.aps.org/doi/10.1103/PhysRevA.93.062513

[36] Gallagher T F 1994 *Rydberg Atoms* (Cambridge, UK: Cambridge University Press)

[37] Alonso A M, Gurung L, Sukra B A D, Hogan S D and Cassidy D B 2018 *Phys. Rev. A* **98**(5) 053417 URL https://link.aps.org/doi/10.1103/PhysRevA.98.053417

[38] Schultz P J and Lynn K G 1988 *Rev. Mod. Phys.* **60**(3) 701–779

[39] Harris F J 1978 *Proceedings of the IEEE* **66** 51–83

[40] Curry S M 1973 *Phys.Rev. A* **7**(2) 447–450

[41] Dermer C D and Weisheit J C 1989 *Phys. Rev. A* **40**(10) 5526–5532

[42] Mills Jr A P and Pfeiffer L 1985 *Phys. Rev. B* **32**(1) 53–57 URL http://link.aps.org/doi/10.1103/PhysRevB.32.53

[43] Mills Jr A P, Shaw E D, Leventhal M, Chichester R J and Zuckerman D M 1991 *Phys. Rev. B* **44**(11) 5791–5799 URL http://link.aps.org/doi/10.1103/PhysRevB.44.5791

[44] Fee M S, Chu S, Mills Jr A P, Chichester R J, Zuckerman D M, Shaw E D and Danzmann K 1993 *Phys. Rev. A* **48**(1) 192–219 URL http://link.aps.org/doi/10.1103/PhysRevA.48.192

[45] Cecchini G G, Jones A C L, Fuentes-Garcia M, Adams D J, Austin M, Membreno E and Mills Jr A P 2018 *Review of Scientific Instruments* **89** 053106 URL https://doi.org/10.1063/1.5017724

[46] Chu S, Mills Jr A P and Hall J L 1984 *Phys. Rev. Lett.* **52**(19) 1689–1692 URL http://link.aps.org/doi/10.1103/PhysRevLett.52.1689

[47] Haas M, Jentschura U D, Keitel C H, Kolachevsky N, Herrmann M, Fendel P, Fischer M, Udem T, Holzwarth R, Hänsch T W, Scully M O and Agarwal G S 2006 *Phys. Rev. A* **73**(5) 052501 URL http://link.aps.org/doi/10.1103/PhysRevA.73.052501

[48] Aghion S *et al* (AEgIS Collaboration) 2016 *Phys. Rev. A* **94**(1) 012507 URL http://link.aps.org/doi/10.1103/PhysRevA.94.012507

[49] Antonello M *et al* (AEgIS Collaboration) 2019 *Phys. Rev. A* **100**(6) 063414 URL https://link.aps.org/doi/10.1103/PhysRevA.100.063414